Ligand Migration in the Truncated Hemoglobin of Mycobacterium tuberculosis

ARTICLE *in* INTERNATIONAL UNION OF BIOCHEMISTRY AND MOLECULAR BIOLOGY LIFE · MARCH 2011

Impact Factor: 3.14 · DOI: 10.1002/iub.438 · Source: PubMed

3 AUTHORS, INCLUDING:

Maxime S Heroux
Medical College of Wisconsin
3 PUBLICATIONS **18** CITATIONS
SEE PROFILE

Kenneth W Olsen
Loyola University Chicago
71 PUBLICATIONS **2,585** CITATIONS
SEE PROFILE

IUBMB *Life*, 63(3): 214–220, March 2011

Research Communication

Ligand Migration in the Truncated Hemoglobin of *Mycobacterium tuberculosis*

Maxime S. Heroux, Anne D. Mohan and Kenneth W. Olsen
Department of Chemistry, Loyola University Chicago, Chicago, IL

Summary

The truncated hemoglobin of *Mycobacterium tuberculosis* (Mt-trHbO) is a small heme protein belonging to the hemoglobin superfamily. Truncated hemoglobins (trHbs) are believed to have functional roles such as terminal oxidases and oxygen sensors involved in the response to oxidative and nitrosative stress, nitric oxide (NO) detoxification, O_2/NO chemistry, O_2 delivery under hypoxic conditions, and long-term ligand storage. Based on sequence similarities, they are classified into three groups. Experimental studies revealed that all trHbs display a 2-on-2 α-helical sandwich fold rather than the 3-on-3 α-helical sandwich fold of the classical hemoglobin fold. Using locally enhanced sampling (LESMD) molecular dynamics, the ligand-binding escape pathways from the distal heme binding cavity of Mt-trHbO were determined to better understand how this protein functions. The importance of specific residues, such as the group II and III invariant W(G8) residue, can be seen in terms of ligand diffusion pathways and ligand dynamics. LESMD simulations show that the wild-type Mt-trHbO has three diffusion pathways while the W(G8)F Mt-trHbO mutant has only two. The W(G8) residue plays a critical role in ligand binding and stabilization and helps regulate the rate of ligand escape from the distal heme pocket. Thus, this invariant residue is important in creating ligand diffusion pathways and possibly in the enzymatic functions of this protein.
IUBMB *Life*, 63(3): 214–220, 2011

Keywords truncated hemoglobin; ligand pathways; *Mycobacterium tuberculosis*; locally enhanced sampling molecular dynamics.

Received 29 December 2011; accepted 1 February 2011
Address correspondence to: Kenneth W. Olsen, Department of Chemistry, Loyola University Chicago, 6525 N. Sheridan Road, Chicago, IL 60626. Tel: +1-773-508-3121. Fax: +1-773-508-3086. E-mail: kolsen@luc.edu kolsen@luc.edu

ISSN 1521-6543 print/ISSN 1521-6551 online
DOI: 10.1002/iub.438

INTRODUCTION

Truncated hemoglobins (trHbs) are small heme proteins found in bacteria, unicellular eukaryotes, and higher plants forming a group within the hemoglobin superfamily (*1*). TrHbs have less than 15% sequence identity when compared with vertebrate and nonvertebrate hemoglobins (*2, 3*). In addition, the primary structure of trHbs display amino acid sequences 20-40 residues shorter than nonvertebrate hemoglobins to which they are scarcely related by sequence similarity (*4*). Crystal studies of trHbs show that the tertiary structure of all trHbs is based on a 2-on-2 α-helical sandwich fold rather than the 3-on-3 α-helical fold of the classical hemoglobin fold (*5, 6*).

Phylogenetic analysis of trHbs sequences shows that these proteins branch into three groups designated I (trHbN), II (trHbO), and III (trHbP). The three groups share less than 30% sequence similarity with each other, while the sequence identity within the same group may be greater than 80% (*4*). Phylogenetic analysis of sequence relationships across and within the three trHb groups shows that within each group, all sequences are orthologous, excluding those sequences in organisms that have two representatives in the same group. In addition, sequences from the same group are paralogous to sequences from another (*7*). In general, paralogues are unlikely to share a common function and, therefore, the three groups of trHbs are expected to consist of proteins that perform distinct roles (*8*). The exceptional coexistence of members of multiple groups in the same organism supports this view.

Biochemical studies have shown that functional roles of trHbs are not conserved across groups I and II trHbs (*9*). For example, the pathogenic bacterium *Mycobacterium tuberculosis* has a group I trHbN, which is expressed during the stationary phase and is thought to be involved in the defense against nitrosative stress, whereas no clear function has been attributed to its group II trHbO, which is expressed throughout the *Mycobacterium* growth phase (*10*). Thus, questions have been raised as to the functions of trHbs. The high oxygen affinity displayed by most trHbs renders their role as oxygen transporters unlikely (*4, 9*). Other functions such as terminal oxidases and oxygen

sensors involved in the response to oxidative and nitrosative stress, nitric oxide (NO) detoxification, O_2/NO chemistry, O_2 delivery under hypoxic conditions, and long-term ligand storage have been proposed (*4, 11–14*).

The overall fold and the relative position of the heme and of the heme contacting residues are similar in group II trHbs. The G, H, E, and B helices of these proteins display the 2-on-2 α-helical fold characteristic of trHbs. Major differences between these trHbOs are observed in the flexible regions between helices (*4, 5, 10, 15*). In contrast to vertebrate and other non-vertebrate hemoglobins, in which most heme pocket residues are conserved, trHbs are characterized by a variability of these residues, especially in the distal side of the heme pocket (*4*). However, there are residues that are conserved within specific groups, such as the W(G8) heme cavity residue, which is conserved between groups II and III trHbs (V/L in group I), that has no counterpart in vertebrate Hbs. An experimental study of the W(G8)F mutation in Mt-trHbO showed that this residue controls ligand binding, as evidenced by a dramatic increase of both association and dissociation rates for O_2 (*16*). Other studies have reported that the W(G8) residue in Mt-trHbO plays a critical role in ligand binding and stabilization as well as regulating the rate of ligand escape out of the distal heme pocket (*10, 14, 16, 17*). Therefore, this article will focus on the effects that the W(G8)F mutant has on the native diffusion pathways and ligand dynamics of Mt-trHbO.

Various studies that have investigated the structure and function of trHbOs have established several key features: low combination and dissociation rates make the diffusion of oxygen as a major function of trHbOs unlikely (*9*). A consensus about the extensive hydrogen bond network within the protein can be found in the literature, with three key residues in trHbO, W(G8), Y(B10), and Y(CD1), forming hydrogen bonds with the distal heme group, controlling ligand access to the heme pocket (*9, 18*). These residues are involved in ligand binding (*9, 16, 18*). There is a change in the orientation of W(G8) in Mt-trHbO between the deoxy and the oxy or carbonmonoxy structures (*9*). The W(G8) may also play a key role in stabilizing the heme group and thus modulating the rate of ligand escape (*9, 16, 19*). Kinetic studies of the W(G8)F and Y(CD1)F proteins have demonstrated that specific residues affect ligand kinetics in different ways. Both the association and dissociation rates of O_2 were dramatically increased in the W(G8)F mutant, whereas only the association rate increased significantly in the Y(CD1)F mutant (*16*). In *Bacillus subtilis* (Bs)-trHbO, Y(B10) has been identified to be the residue directly hydrogen bonded to the ligand, while Y(CD1) is the corresponding residue in Mt-trHbO (*19*). Several tunnels and cavities have been identified in trHbOs (*9, 16, 18, 19*). Residues lining the tunnels are hydrophobic and are conserved throughout each trHb family. These residues play major roles in the ligand pathways (*9, 16, 18, 19*). Different residues may determine which ligand will be bound or modulate the rate of binding and diffusion (*19*). In Mt-trHbN, two conformations of Y(B10) and Q(E11) side chains within the hydrogen-bond network were observed, depending on the presence or absence of O_2 (*20–22*). Y(B10) and Q(E11) in turn control the dynamics of F(E15), which is restricted in the deoxy-Mt-trHbN but can fluctuate between two conformations in the oxy state (*20–22*). Similar conformational changes have been suggested in the mechanism for ligand binding in Bs-trHbO, where W(G8) and Q(E11) are thought to block the long tunnel, which is topographically positioned toward the helices B and E, running parallel to the long protein axis but may rearrange to open it (*18*). W(G8) also blocks a potential short tunnel between the G and H helices (*19*), whereas the short tunnel between the CE-turn and the heme is open. The opening of the long tunnel in Mt-trHbN is mediated by F(E15) (*18*). However, there are still questions regarding the functional role of specific residues in tr-HbOs and their role overall, because different species in the family of trHbO have been shown to use different strategies for ligand binding and release (*18*).

Using locally enhanced sampling (LESMD) molecular dynamics (*23, 24*), the goals of this work are to determine the ligand escape pathways from the distal heme cavity of Mt-trHbO and how the W(G8)F mutation might effect those dissociation pathways. This study will provide a better understanding of how the native trHbs function and the potential effects that the W(G8)F mutation might have on the function of this trHb.

EXPERIMENTAL PROCEDURES

The atomic coordinates of Mt-trHbO used in the simulations were obtained from the Protein Data Bank (*25*). The X-ray diffraction structure for Mt-trHbO (*10*) at 2.11 Å resolution was used (PDBid: 1ngk). The A chain structure was used in this molecular dynamics study. Protein cavities of Mt-trHbO were identified by means of an internal surface analysis performed with CAST P (*26*) using a 1.4 Å probe radius. All simulations were performed using NAMD (*27*) and data analysis was done using VMD (*28*). Molecular figures were generated using VMD. The W(G8)F mutation was introduced in the Mt-trHbO structure using the molecular graphics program Swiss-PDBViewer (*29*). The average root mean square deviation (RMSD) on all protein atoms was calculated compared to the X-ray structure for the wild-type and mutated protein structures over their entire trajectory simulations using the VMD RMSD trajectory application (*28*).

The LESMD calculations were performed using version 2.6 of the program NAMD (*27*) and the CHARMM27 all atom force field (*30*). The initial structure had a six-coordinated heme iron with a cyanide ligand as the sixth ligand. To obtain proteins with an O_2 ligand in the heme distal cavity necessary for oxygen transport studies, oxygen replaced the cyanide ion and the iron was parameterized as Fe(II), as found in the CHARMM27 force field using the PLO2 patch (*30*). The Mt-trHbO molecule was immersed into a TIP3 water box. Periodic boundary conditions were used. The cutoffs for nonbonding (van der Waals and electrostatic) interactions were 12 Å. The switch distance was 10 Å, and 1.0 1–4 scaling factor was used.

LESMD is a mean field approach enhancing the sampling of the conformational space due to the presence of multiple copies and their higher (with respect to "cold" protein) effective temperature (*23, 24*). Fifteen copies of oxygen were used in all of these simulations. These copies do not interact with each other, and interact with the rest of the system with a scaling factor of 1/15. During the simulation, the copies are free to explore different regions of conformational space, thereby, increasing the statistical sampling. The barriers to transitions in a LES system are reduced when compared with the original system. The protein with 15 copies of bound O_2 ligands was equilibrated at constant temperature (310 K) and pressure (1 atm). Production simulations were performed at constant volume and temperature with 15 copies of unbound O_2 ligands. The solvated Mt-trHbO system used in these simulations had over 15,000 atoms. Each trajectory was 10 ns long or ran until all of the O_2 molecules diffused out of the protein interior into the solvent.

For the analysis, VMD (*28*) was used. Residues involved in short range interactions with the ligands were obtained for collisions between the O_2 ligands and the protein, defined as any interatomic distance less than 2.5 Å.

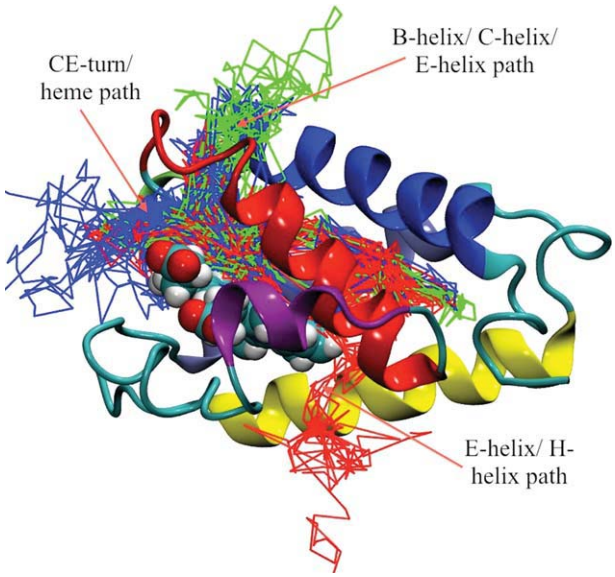

Figure 1. Molecular model of the diffusion pathways of wild-type Mt-trHbO. The major pathway observed was the CE-turn/heme tunnel (blue trajectory). The two minor pathways observed were the E-helix/H-helix tunnel (red trajectory) and the B-helix/C-helix/E-helix tunnel (green trajectory). [Color figure can be viewed in the online issue, which is available at wileyonlinelibrary.com.]

RESULTS

Protein Cavities of Mt-trHbO using CAST P

Internal surface analyses performed using the CAST P program identified four major cavities, in addition to the heme pocket. It was expected that these cavities would be used on the escape routes. The distal heme cavity is lined by Y23, Y36, A44, L48, and W88. Two hydrophobic internal cavities that might be used as holding areas for oxygen were found. The first internal cavity was defined by F15, I18, V19, L52, M92, L112, and L166. The second one was F5, V9, T14, F15, I18, L104, and L112. The two external pockets were less hydrophobic and might form oxygen release sites. The first external pocket was linked to the second inner cavity and contained residues A8, V9, T103, L104, D105, and H108. The second external pocket was near the heme and contained residues R33, Y36, P37, E38, D39, and L41.

Calculated RMSD Values of the Wild-Type and Mutant Mt-trHbO

The average RMSD calculated for all protein atoms of the wild-type Mt-trHbO over their entire trajectory simulations was 1.4 Å, respectively. The average RMSD calculated for the W(G8)F-mutated Mt-trHbO protein over their entire trajectory simulations was1.5 Å.

LESMD Simulations of Mt-trHbO and its W(G8)F Mutant

In this article, pathway tunnels are defined by the residues and helices through which the O_2 ligands escape on their way into the solvent. Key residues were found to be common to specific O_2 migration pathways. Fluctuations of specific sidechains, which open transient gates to cavities allowing for ligand diffusion were observed using VMD and will be labeled as "gates" throughout this paper.

O_2 Migration and Diffusion Pathway Tunnels of Mt-trHbO

All of the 15 O_2 ligands observed left the protein within 10 ns in the LESMD simulation. In the wild-type protein, three distinct diffusion pathway tunnels were observed (Fig. 1). The predominant escape route observed was the CE-turn/heme pathway. The two minor pathways observed were the E-helix/H-helix tunnel and the B-helix/C-helix/E-helix tunnel. The residues that line these pathway tunnels and their corresponding gates are shown in Fig. 2. During the duration of the simulation, ligands explored the binding distal heme pocket and the internal and external cavities of Mt-trHbO. The first two ligands were released via the CE-turn/heme pathway at 0.6 ns into the simulation. In the next 1.7 ns, seven oxygens exited the protein: four of these ligands diffused via the CE-turn/heme pathway, one by the E-helix/H-helix pathway tunnel, and two via the B-helix/C-helix/E-helix pathway tunnel. During the next 4.3 ns, five oxygen ligands diffused out of the protein. Three of these five ligands diffused out via the E-helix/H-helix pathway tunnel, whereas one ligand exited via the CE-turn/heme pathway and one ligand by the B-helix/C-helix/E-helix pathway tunnel. The last ligand diffused out of Mt-trHbO by the B-helix/C-helix/E-helix pathway tunnel at 7.7 ns into the simulation.

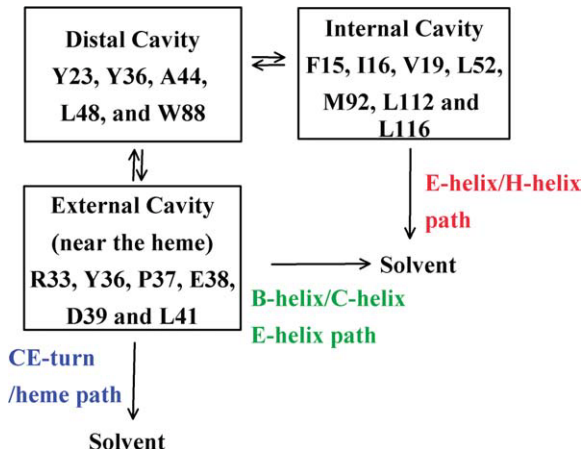

Figure 2. Scheme of the diffusion pathways of wild-type Mt-trHbO. [Color figure can be viewed in the online issue, which is available at wileyonlinelibrary.com.]

Of the 15 O_2 ligands, eight of them diffused out of the protein via the CE-turn/heme pathway, seven of them early in the simulation, and one much later. The time that these eight ligands spent within the protein was concentrated in the distal heme pocket and the external cavity near the heme. Throughout the simulation, these eight ligands traveled from the distal heme pocket to the external cavity and then back to the distal heme pocket, by passing residues Y36 and L41. Most of these ligands diffused out of the protein and into the solvent between residues P37 and D40, although two of them remained in contact with the surface of the protein and left it closer to F78. The weighted percentage of time spent by the eight ligands in the distal heme pocket and the external cavity near the heme are 60 and 40%, respectively.

Four of the 15 O_2 ligands diffused out of the protein via the E-helix/H-helix tunnel. Starting at the distal heme pocket, the four ligands traveled to the first inner cavity by passing residues V19 and L48. From the first internal cavity the ligands would migrate back to the distal heme pocket between residues V19 and L48 throughout their time in the protein. The four ligands never visited the second internal cavity. The ligands diffused out of the protein and into the solvent between residues Y55, Y115, M118, and A119. The weighted percentage of time spent by the four ligands at the heme distal pocket and the first inner cavity were 70 and 30%, respectively.

Only three of the 15 O_2 ligands diffused out of the protein via the B-helix/C-helix/E-helix pathway. Two of these ligands always remain within the distal heme pocket and the external cavity identified near the heme, while one of them diffused into the internal cavity before returning to the distal cavity to exit. Throughout the simulation, these three ligands traveled from the distal heme pocket to the external cavity and then back to the distal heme pocket, by passing residues Y36 and L41. The ligands diffused out of the protein and into the solvent by passing between residues Y23, L41, and A42. Thus, the initial escape from distal heme cavity is the same for this pathway and the CE-turn/heme pathway, but the exit to the solvent from the external cavity is quite different. The weighted percentage of time spent by the three ligands in the distal heme pocket and the external cavity near the heme are 40 and 60%, respectively.

Collision counts between oxygen ligands and the protein for the E-helix/H-helix, CE-turn/heme, and B-helix/C-helix/E-helix paths observed in the simulation trajectory show that L41 and W88 affect ligand diffusion out of Mt-trHbO the most for all of the observed pathways. These results suggest that these two residues may be the most critical in determining the overall diffusion routes for ligands out of Mt-trHbO.

O_2 Migration and Diffusion Pathway Tunnels of Mt-trHbO W(G8)F Mutant

In the W(G8)F (residue 88) Mt-trHbO mutant, all of the 15 O_2 ligands observed left the protein on a 10 ns timescale. Two distinct diffusion pathways were observed (Fig. 3). The major pathway observed was the E-helix/H-helix pathway. The other pathway observed in the W(G8)F Mt-trHbO mutant was the CE-turn/heme tunnel. The residues that line these pathway tunnels and their corresponding gates are shown in Fig. 4. This is interesting because the major CE-turn/heme tunnel observed in the native Mt-trHbO was shown to be a minor diffusion pathway in the W(G8)F Mt-trHbO mutant, and the B-helix/C-helix/E-helix pathway was not observed in simulations of the mutant protein. During the duration of the simulation, ligands explored the binding distal heme pocket, specific residue pockets, and the

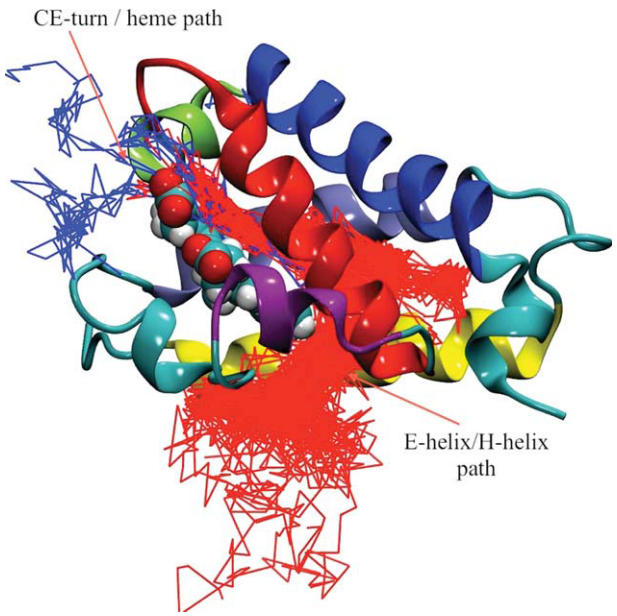

Figure 3. Molecular model of the diffusion pathways of W(G8)F mutant of Mt-trHbO. The major pathway observed was the E-helix/H-helix tunnel (red trajectory). The only minor pathway observed was the CE-turn/heme tunnel (blue trajectory). [Color figure can be viewed in the online issue, which is available at wileyonlinelibrary.com.]

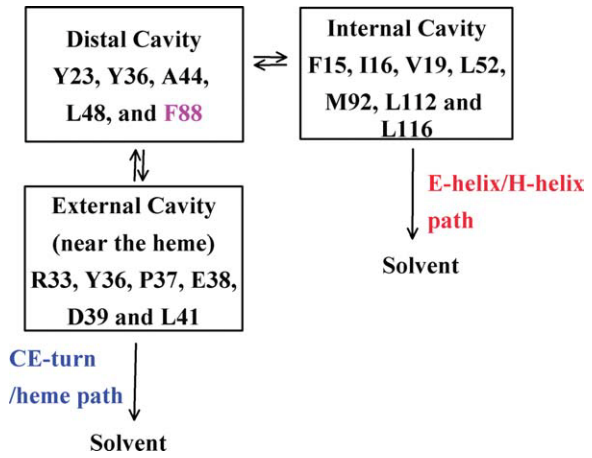

Figure 4. Scheme of the diffusion pathways of W(G8)F mutant of Mt-trHbO. [Color figure can be viewed in the online issue, which is available at wileyonlinelibrary.com.]

inner and external cavities of the mutant protein. Five ligands were released via the CE-turn/heme path and one via the E-helix/H-helix path less than 0.3 ns into the simulation. The exit residues for the CE-turn/heme ligands were V35, P37, and F78, while the lone E-helix/H-helix ligand exited near L115 and A119. In the next 2 ns, eight ligands exited the protein by the E-helix/H-helix route. During the next 1 ns, the final ligand diffused into the solvent via the E-helix/H-helix pathway. Within 3.8 ns, all of the 15 oxygens had escaped the Mt-trHbO mutant. Thus, the ligands escaped much more rapidly in this mutant than in the native protein.

Of the 15 O_2 ligands, 10 of them diffused out of the protein via the E-helix/H-helix tunnel. The residues that define this pathway share the same residues that define the E-helix/H-helix route of the native Mt-trHbOs; however, the flux of oxygen molecules through this pathway is greater in the W(G8)F mutant protein due to the lack of the B-helix/C-helix/E-helix tunnel in the mutant protein. Throughout the simulation, these 10 ligands traveled from the distal heme pocket to the first inner cavity and then back to the distal heme pocket, by passing residues V19 and L48. They never visited the second internal cavity. The E-helix/H-helix route exits the protein near F48, Y55, W56, L71, L116, M118, A119, and S122. The E-helix/H-helix ligands in the W(G8)F Mt-trHbO mutant span more regions of the protein than the ones leaving via the CE-turn/heme pathway (Fig. 3).

Five of the 15 O_2 ligands diffused out of the protein via the CE-turn/heme tunnel. The residues that define this pathway share some of the same residues that define the CE-turn/heme pathway of the native Mt-trHbO. All of the time that the five ligands spent within the protein was concentrated solely in the starting distal heme pocket. These five ligands diffused out of the protein and into the solvent between residues P37, A44, and R47.

Collision counts for the W(G8)F Mt-trHbO mutant observed in the simulation show that most involved residues are L52, Y55, L71, and L116 for the E-helix/H-helix path and P37 and A44 for the CE-turn/heme path.

DISCUSSION

Using VMD software, traces of every O_2 ligand were observed for all trajectories in these LESMD simulations of Mt-trHbO and its W(G8)F mutant. The main questions addressed in this article are what are possible diffusion pathway tunnels for O_2 ligands from the distal heme pocket into the solvent for Mt-trHbO and its mutant? Are they the same? Is there only one dominant pathway or several? Which residues may affect ligand diffusion out of Mt-trHbO and the mutants? The LESMD simulations presented here suggest answers to these questions.

The calculated average RMSD on all protein atoms for the native Mt-trHbO and the mutant over their entire trajectory simulations suggest that the protein structures were stable throughout their trajectory simulations ($<$1.5 Å). In addition, these values show a lack of large protein movement while the O_2 ligands diffuse from the heme out into the solvent. Thus, the observed paths are pre-existing or due to local structural fluctuations and not created by larger conformational changes.

Oxygen dissociation rates are thought to be well explained by the O_2 affinities for the hemes, and their O_2 pathway networks have very little effect on these rates (*32*). Thus, the effect of the O_2 pathway shapes and locations would be of minor importance relative to the effect of the bound ligand's environment at the heme (*32*). However, mutations can greatly change association and dissociation rates (*16*). In addition, the different pathways observed in globins may have important roles in enzymatic functions such as kinetic proofreading as a means to increase or decrease the selectivity of protein binding to various gases (*33*) or as a means to promote specific reactions catalyzed by certain proteins (*34*). Although O_2 dissociation rates cannot be predicted using the LESMD method, the combination of kinetic studies and LESMD simulations can provide better insight into the molecular processes. In addition, identification of the residues forming these pathways can be used to plan pathway-altering mutations inside proteins. By mutating residues that have a predisposition to create O_2 favorable regions, such as large hydrophobic residues and those possessing aromatic rings (*32*), to those that do not, the kinetics of oxygen binding and escape could be changed.

Guertin and co-workers (*16*) performed guanidine denaturation experiments to determine the impact of the W(G8)F substitution on the protein stability of Mt-trHbO. This study found that the guanidine concentration required to denature half of the proteins was 3.0 and 2.6 for the wild-type and the mutated W(G8)F Mt-trHbO structures, respectively. Thus, the W(G8)F mutation slightly decreases protein stability. The calculated RMSD values for the wild-type and mutated forms of Mt-trHbO show that the mutation does not significantly affect the backbone conformation and the mutated F side chain closely matches the conformation adopted by W(G8) in the wild-type

protein in the simulations presented here. These results are consistent with the experimental finding of only slightly decreased stability.

The different ligand diffusion pathways observed in globins may have important implications for the potential enzymatic functions of these proteins. Specific mutations can cause drastic changes in both kinetic rate and diffusion pathways, such as shown by kinetics studies by Ouellet and co-workers (*16*) and molecular dynamics simulations shown here. Changing the key residue W(G8) in Mt-trHbO to an F changed the major pathway through the CE-turn/heme in the native trHb to a minor one in the mutant. This point mutation shifted the major pathway to the E-helix/H-helix tunnel. These findings agree with the results published by Boechi et al. (*35*) who also found the major ligand escape to be through the CE-turn/ heme path in the wild-type trHbO and further reported that mutating key residues changes the ligand escape pathways. It should be noted, however, that the number of ligands that escape through a specific pathway during a LESMD simulation does not necessarily correspond to the number of channel opening events. For example, in the W(G8)F mutant five ligands escape early in the simulation via the CE-turn/heme tunnel, but this may represent only one opening of that channel since the ligands leave at the same time. One of the surprising changes due to the mutation seen in these simulations is the disappearance of the B-helix/C-helix/E-helix tunnel. In the wild-type protein Y(CD1) is initially making a hydrogen-bond to W(G8) and blocks this route. When that hydrogen-bond breaks during the simulation, Y(CD1) can shift to a new position due to a slight rotation and reorientation of the C-helix. The Y(CD1) can then form hydrogen-bonds from the hydroxyl group to solvent and to the main-chain carbonyl group of R79 on the FG-loop. The rest of Y(CD1) remains buried. This movement opens the B-helix/C-helix/E-helix channel, which is not seen in the W(G8)F mutant protein. In the mutant protein, the interactions between F(G8) and Y(CD1) are hydrophobic, and the Y(CD1) is shifted slightly away from the CE-turn compared to its position in the wild-type structure. In the mutant protein, the Y(CD1) remains trapped in this position during the entire simulation blocking the B-helix/C-helix/E-helix channel. In Bs-trHbO, Q(E11) helps stabilize the bound ligand (*18*), but that position is a leucine in Mt-trHbO, leading to different dynamics in the ligand binding site. In the simulations described here, when the hydrogen-bond between W(G8) and Y(CD1) breaks, new escape pathways are possible. In the W(G8)F mutant, this hydrogen-bond cannot form, allowing easier escape via the E-helix/H-helix tunnel. Thus, W(G8) acts as a gatekeeper for ligand diffusion in the wild-type protein. The pathways described by Boechi et al. (*18*) for Bs-trHbO have also been seen in the simulations presented here for Mt-trHbO, but the additional simulations of the W(G8)F mutant protein provide a possible atomic explanation for the observed kinetic changes (*16*).

The residues that are in contact with the oxygen molecules when they exit the protein are almost always hydrophobic, even though they are on the surface of the protein. Tyrosine, phenylalanine, isoleucine, leucine, methionine, and proline are all involved in the different surface exit points. It is likely that these are also the entrance points for nonpolar gases. During these simulations, the tendency of the oxygen molecules to linger near these hydrophobic surface residues was often observed.

Although the W(G8)F mutation did not significantly affect the conformation or the structural stability of Mt-trHbO, this point mutation did affect the diffusion pathways. Phenylalanine is still a large residue, but it is smaller than tryptophan. It also lacks the ability to form a hydrogen bond. As a result of the mutation, the B-helix/C-helix/E-helix path was blocked by a shift in the position of Y(CD1). The mutation also made escape via the E-helix/H-helix easier. In addition, more oxygen molecules re-entered the protein and the distal cavity from the solvent during the simulations of the W(G8)F mutant than did during the wild-type simulations. Thus, the invariant W(G8) residue is important not only in playing critical roles in ligand binding and stabilization and in regulating the rate of ligand escape out of the distal heme pocket, as reported by other studies (*16*) but also in creating stable diffusion pathways. By determining what ligand diffusion paths exist within the protein, the W(G8) could be important in the enzymatic functions tr-HbOs promote.

REFERENCES

1. Watts, R. A., Hunt, P. W., Hvitved, A. N., Hargrove, M. S., Peacock, W. J., and Dennis, E. S. (2001) A hemoglobin from plants homologous to truncated hemoglobins of microorganisms. *PNAS* **98**, 10119–10124.
2. Couture, M., Chamberland, H., St. Pierre, B., Lafontaine, J., and Guertin, M. (1994) Nuclear genes encoding chloroplast hemoglobins in the unicellular green alga *Chlamydomonas eugametos*. *Mol. Gen. Genet.* **243**, 185–197.
3. Moens, L., Vanfleteren, J., Van de Peer, Y., Peeters, K., Kapp, O., Czeluzniak, J., Goodman, M., Blaxter, M., and Vinogradov, S. (1996) Globins in nonvertebrate species: dispersal by horizontal gene transfer and evolution of the structure-function relationships. *Mol. Biol. Evol.* **13**, 324–333.
4. Wittenberg, J., Bologhnesi, M., Wittenberg, B., and Guertin, M. (2002) Truncated hemoglobins: a new family of hemoglobins widely distributed in bacteria, unicellular eukaryotes, and plants. *J. Biol. Chem.* **277**, 871–874.
5. Milani, M., Pesce, A., Ouellet, Y., Ascenzi, P., Guertin, M., and Bolognesi, M. (2001) *Mycobacterium tuberculosis* hemoglobin N displays a protein tunnel suited for O_2 diffusion to the heme. *EMBO J.* **20**, 3902–3909.
6. Perutz, M. F. (1979) Regulation of oxygen affinity of hemoglobin: influence of structure of the globin on the heme iron. *Annu. Rev. Biochem.* **48**, 327–386.
7. Tatusov, R. L., Koonin, E. V., and Lipman, D. J. (1997) A genomic perspective on protein families. *Science* **278**, 631–637.
8. Vuletich, D. A. and Lecomte, J. T. J. (2006) A phylogenetic and structural analysis of truncated hemoglobins. *J. Mol. Evol.* **62**, 196–210.
9. Ouellet, H., Juszczak, L., Dantsker, D., Samuni, U., Ouellet, Y. H., Savard, P. Y., Wittenberg, J. B., Wittenberg, B. A., Friedman, J. M., and Guertin, M. (2003) Reactions of *Mycobacterium tuberculosis* truncated hemoglobin O with ligands reveal a novel ligand-inclusive hydrogen bond network. *Biochemistry* **42**, 5764–5774.

10. Milani, M., Savard, P. Y., Ouellet, H., Ascenzi, P., Guertin, M., and Bolognesi, M. (2003) A TyrCD1-TrpG8 hydrogen bond network and a TyrB10-TyrCD1 covalent link shape the heme distal site of *Mycobacterium tuberculosis* hemoglobin O. *Proc. Natl. Acad. Sci. USA* **100**, 5766–5771.
11. Dikshit, R. P., Dikshit, K. L., Liu, Y. X., and Webster, D. A. (1992) The bacterial hemoglobin from *Vitreoscilla* can support the aerobic growth of *Escherichia coli* lacking terminal oxidases. *Arch. Biochem. Biophys.* **293**, 241–245.
12. Couture, M., Yeh, S. R., Wittenberg, B. A., Wittenberg, J. B., Ouellet, Y., Rousseau, D. L., and Guertin, M. (1999) A cooperative oxygen-binding hemoglobin from *Mycobacterium tuberculosis*. *Proc. Natl. Acad. Sci. USA* **96**, 11223–11228.
13. Ouellet, H., Ouellet, Y., Richard, C., Labarre, M., Wittenberg, B. A., Wittenberg, J. B., and Guertin, M. (2002) Truncated hemoglobin HbN protects *Mycobacterium bovis* from nitric oxide. *Proc. Natl. Acad. Sci. USA* **99**, 5902–5907.
14. Giangiacomo, L., Ilari, A., Boffi, A., Morea, V., and Chiancone, E. (2005) The truncated oxygen-avid hemoglobin from *Bacillus subtilis*: X-ray structure and ligand binding properties. *J. Biol. Chem.* **280**, 9192–9202.
15. Ilari, A., Kjelgaard, P., Von Wachenfeldt, C., Cttacchio, B., Chiancone, E., and Boffi, A. (2006) Structure and ligand binding properties of the hemoglobin from *Geobaccilus stearothermophilus*. *Arch. Biochem. Biophys.* **457**, 85–94.
16. Ouellet, H., Milani, M., LaBarre, M., Bolognesi, M., Couture, M., and Guertin, M. (2007) The roles of Tyr(CD1) and Trp(G8) in *Mycobacterium tuberculosis* truncated hemoglobin O in ligand binding and on the heme distal site architecture. *Biochemistry* **46**, 11440–11450.
17. Guallar, V., Changyuan, L., Borrelli, K., Egawa, T., and Yeh, S. R. (2009) Ligand migration in the truncated hemoglobin-II from *Mycobacterium tuberculosis*: the role of G8 tryptophan. *J. Biol. Chem.* **284**, 3106–3116.
18. Boechi, L., Manez, P. A., Luque, F. J., Marcelo A. M., and Estrin, D. A. (2010) Unraveling the molecular basis for ligand binding in truncated hemoglobins: the trHbO *Bacillus subtilis* case. *Proteins* **78**, 962–970.
19. Pesce, A., Nardini, M., Milani, M., and Bolognesi, M. (2007) Protein structure in the truncated (2/2) hemoglibin family. *IUBMB Life* **59**, 535–541.
20. Daigle, R., Guertin, M., and Lague, P. (2009) Structural characterization of tunnels in Mt-trHbN from molecular dynamics simulations. *Proteins* **75**, 735–747.
21. Crespo, A., Marti, M. A., Kalko, S. G., Morreale, A., Orozco, M., Gelpi, J. L., Luque, F. J., Estrin, D. A. (2005) Theoretical study of the truncated hemoglobin HbN: exploring the molecular basis of the NO detoxification mechanism. *J. Am. Chem. Soc.* **127**, 4433–4444.
22. Bidon-Chanal, A., Marti, M. A., Crespo, A., Milani, M., Orozco, M., Bolognesi, M., Luque, F. J., Estrin, D. A. (2006) Ligand-induced dynamical regulation of NO conversion in *Mycobacterium tuberculosis* truncated hemoglobin-N. *Proteins* **64**, 457–464.
23. Elber, R. and Karplus, M. (1990) Sampling in molecular dynamics: use of the time-dependent Hartree approximation for a simulation of carbon monoxide diffusion through myoglobin. *JACS* **112**, 9161–9175.
24. Golden, S. D. and Olsen, K. W. (2008) Identification of ligand binding pathways in truncated hemoglobins using locally enhanced sampling molecular dynamics. *Methods Enzymol.* **437**, 457–473.
25. Berman, H. M., Westbrook, J., Feng, Z., Gilliland, G., Bhat, T. N., Weissig, H., Shindyalov, I. N., and Bourne, P. E. (2000) The Protein Data Bank. *Nucleic Acid Res.* **28**, 235–242.
26. Liang, J., Edelsbrunner, H., and Woodward, C. (1998) Anatomy of protein pockets and cavities: measurement of binding site geometry and implications for ligand design. *Protein Sci.* **7**, 1884–1897.
27. Phillips, J. C., Braun, R., Wang, W., Gumbart, J., Tajkhorshid, E., Villa, E., Chipot, C., Skeel, R. D., Kale, L., and Schulten, K. (2005) Scalable molecular dynamics with NAMD. *J. Comp. Chem.* **26**, 1781–1802.
28. Humphrey, W., Dalke, A., and Shulten, K. (1996) VMD—Visual Molecular Dynamics. *J. Mol. Graphics* **14**, 33–38.
29. Guex, N. and Peitsch, M. C. (1997) SWISS-MODEL and the Swiss-PdbViewer: an environment for comparative protein modeling. *Electrophoresis* **18**, 2714–2723.
30. MacKerell, A. D. Jr., Feig, M., and Brooks, C. L., III. (2004) Extending the treatment of backbone energetics in protein force fields: limitations of gas-phase quantum mechanics in reproducing protein conformational distributions in molecular dynamics simulations, *J. Comp. Chem.* **25**, 1400–1415.
31. Roitberg, A. and Elber, R. (1991) Modeling side chains in peptides and proteins: application of the locally enhanced sampling and simulated annealing methods to find minimum energy conformations. *J. Chem. Phys.* **95**, 9277–9287.
32. Cohen, J. and Schulten, K. (2007) O_2 migration pathways are not conserved across proteins of a similar fold. *Biophys. J.* **93**, 3591–3600.
33. Radding, W. and Phillips, G. N. Jr. (2004) Kinetic proofreading by the cavity system of myoglobin: protection from poisoning. *Bioessays* **26**, 422–433.
34. Brunori, M. and Gibson, Q. H. (2001) Cavities and packing defects in the structural dynamics of myoglobin. *EMBO Rep.* **2**, 676–679.
35. Boechi, L., Marti, M. A., Milani, M., Bolognesi, M., Luque, F. J., Estrin, D. A. (2008) Structural determinants of ligand migration in *Mycobacterium tuberculosis* truncated hemoglobin O. *Proteins* **73**, 372–379.